

Design and Build of Masked Face Identification System and IoT-Based Body Temperature Measurement

I P.A. Bayupati ^{a,*}, Aditya Ersapramana ^a, I Putu Arya Dharmadi ^a

^a Department of Engineering, Udayana University, Badung, Bali, Indonesia

Corresponding author: *bayupati@unud.ac.id

Abstract—The new normal is an era in the behavior changed to obstruct the spread of COVID-19, such as decreasing people's mobility, body temperature measuring, mandatory masking, and getting a COVID-19 vaccine regularly. This study develops an identification system based on the Internet of Things through facial biometrics and temperature measurement. Face identification is divided into two main steps: face detection and identification. Face detections used the Framework YOLOv5, in which the systems can detect masked and without masked faces. Pre-trained VGG-face is used for face identification for feature extraction and produces a 2622-dimensional vector. The feature extraction result is calculated as the distance similarity with the features stored in the Database using Euclidean distance. Temperature measurement utilizes IoT by using the NodeMCU ESP8266 and the MLX90614 sensor. NodeMCU ESP8266 is a microcontroller equipped with a WI-FI module to send temperature data so measurements can be delivered wirelessly. The MLX90614 sensor measures body temperature at a 40 – 60 cm distance from the Sensor. Calibration of the sensor used Two-point Calibration, so a trim error rate level is produced. The result successfully identified the face with the F1 score of 92% without a masked face and 73% for a masked face. The body temperature was measured using the MLX90614 sensor produced an error rate of 0.1°C after calibration. In the future, this system can be further developed and utilized for other sectors, such as the medical and security sectors.

Keywords— Face identification; feature extraction; internet of things; MLX90614; temperature measurement; YOLO; VGG-Face.

Manuscript received 13 Jun. 2022; revised 23 Jan. 2023; accepted 21 May 2023. Date of publication 31 Aug. 2023.
IJASEIT is licensed under a Creative Commons Attribution-Share Alike 4.0 International License.



I. INTRODUCTION

Severe acute respiratory syndrome coronavirus 2 (SARS-CoV-2) or COVID-19, is a disease that attacks the human respiratory system [1]. COVID-19 has been spreading rapidly, which results in the immobility of everyday human activities. The spread of COVID-19 has forced almost all countries to make decisions for lockdown or regional quarantine. People with COVID-19 may experience fever, dry cough, and difficulty breathing [2], [3]. The COVID-19 pandemic has undoubtedly forced the entire world community to adopt a new lifestyle to continue carrying out their activities, thus making many changes and developing technology to assist community activities, one of which is the biometric attendance system with temperature measurement. The biometric system has its characteristics and uniqueness for every human being. Because of this, the biometric system can be used as a security system [4].

The face is a biometric system that is often used because it is easy to use and has a high level of security. The use of the

face as a biometric recognition was first used in 1960 to determine the locale feature of a person [5]. Facial biometric identification research is developed with various new methods [6]–[9].

Face identification is carried out in two stages: face detection and face recognition. Face detection is a process of finding faces in an image [10]. Research on face detection has been carried out using various object detection models, one of which is the Convolutional Neural Network (CNN) [11]. Convolutional Neural Network is a good model used in looking for objects [12]. One of the popular CNN models used in object detection is the YOLO model [13]–[15]. Face identification is a process based on a person's facial characteristics [16]. Face identification is made by finding features in the faces. The feature extraction process is a challenge regarding appearance because good feature extraction can improve facial accuracy. In recent years, methods have been developed that can perform feature extraction. The feature extraction model mainly uses CNN as its architecture [17], [18]. The feature extraction results are then matched, and several methods are used, such as PCA

[19], SVM [20], Euclidean distance, and cosine similarity [21]. The COVID-19 pandemic has significantly impacted the face identification process caused by masks that partially cover the face. Several studies have been carried out on this issue, Deng, et al. [22] developed a masked face identification algorithm based on large-margin cosine loss where this method utilizes the part of the face that is not covered by the mask. Ud Din, et al. [23] developed a method of removing masks from the face using a GAN-based network.

Prevention of COVID-19 can also be done by measuring body temperature. Human body temperature is one indicator of determining human health status [24]. Human body temperature is usually measured in the armpit, mouth, rectum, ear, or forehead. Each temperature measurement area has a different average temperature [25]. The COVID-19 pandemic has led to the development of a contactless body temperature measurement system. The development of contactless body temperature measurement aims to reduce the potential for direct contact with objects that have the potential to spread the COVID-19 virus. One of the methods for measuring body temperature is using the Internet of Things, which can utilize a touchless body temperature measurement using a temperature sensor [26]–[28].

This study aims to create a masked face attendance system. The attendance system is built with two integrated systems: the attendance system and body temperature measurement. Research focuses on developing a contactless attendance system to overcome the spread of COVID-19. The main challenge in this research is how the system can identify a masked face using training data face without a mask. Face identification is carried out in two stages: face detection and face identification. The face detection stage uses the YOLOv5 Framework. The face identification stage begins by extracting features from the detected faces using the pre-trained VGG-Face. This feature extraction will produce 2622 dimensional vectors. The feature extraction result is then normalized, and similarity comparison is performed using Euclidean Distance. The Internet of Things used in this research utilizes an infrared sensor module to measure temperature and a Wi-Fi module for data transmission. The Results are stored in the Database. The development of this attendance system is expected to be efficiently used in the new normal.

II. MATERIALS AND METHOD

The proposed system has two integrated systems: a facial identification system and body temperature measurement. The system design can be seen in Figure 1, which shows the entire process in the system. The input image for face identification with a resolution of 640*480 is captured using a smartphone camera. Then face detection is performed using YOLOv5. The result of face detection is performed feature extraction using the pre-trained VGG-Face model. Feature extraction will produce 2622 dimensional vectors which are used for distance similarity using Euclidean distance.

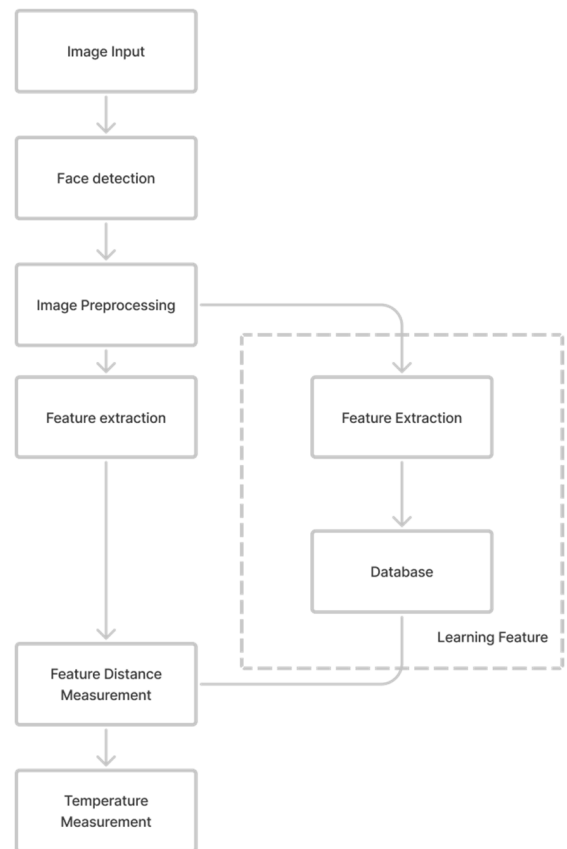


Fig. 1 Design system of face identification and temperature measurement

Figure 2 shows a schematic diagram of the whole system. The body temperature measurement system uses the NodeMCU ESP8266 board and the MLX90614 sensor. The body temperature measurement and facial assessment systems are integrated by sending body temperature data to the facial system using a Wi-Fi network. The body and facial temperature measurements will be stored in the Database as attendance data.

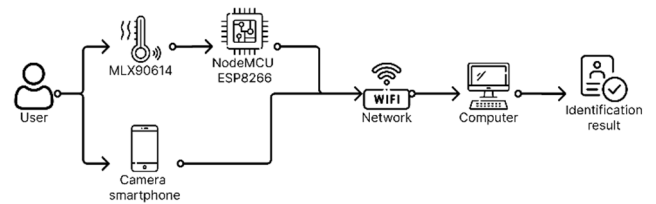


Fig. 2 Physical Implementation System

A. Face Identification

Face identification is done using the YOLOv5 framework with the YOLOv5s model. Yolo is a state-of-the-art, real-time object detector, and YOLOv5 is based on YOLOv1-YOLOv4 [15]. The training process is carried out using a face dataset and face masks that have been labeled and marked with bounding boxes which are stored in different files. The YOLOv5 architecture can be seen in Figure 3.

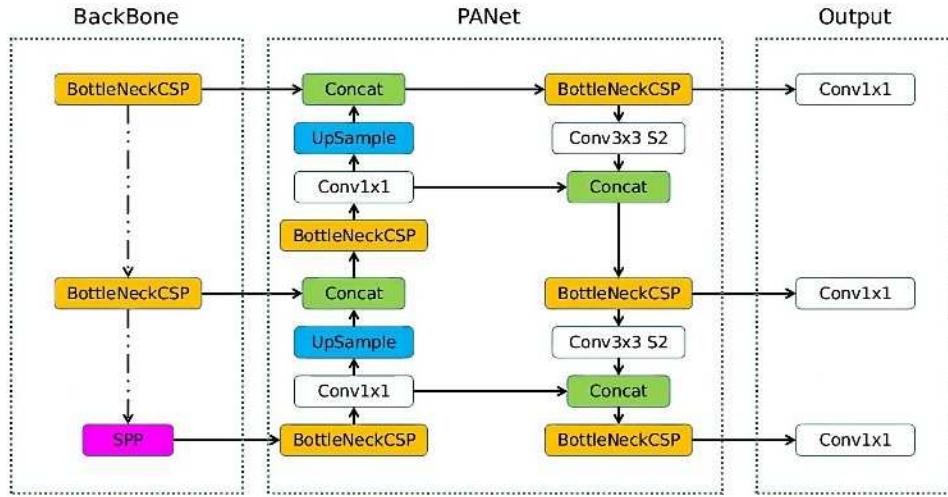


Fig. 3 The architecture of YOLOv5

The way the YOLOv5 framework works starts from the input layer to the backbone layer. CSPDarknet acts as a backbone to extract features from the input image [29]. The result of feature extraction is continued to the neck. PANet acts as a neck to create a feature pyramid. This pyramid feature helps the model perform object scaling. The head or output section is the final part of the detection object. The Yolo Layer acts as the head layer to anchor boxes of detected objects and produces output vectors of class probabilities and bounding boxes. The YOLOv5 architectural configuration used in this study uses the YOLOv5s configuration. YOLOv5s is a model configuration with the smallest depth multiple and width multiple values. This value affects the depth of the model and channel layer in learning the object detection model [29].

B. Feature Extraction

Facial features in this study were performed using a 5-point face feature extraction. Feature extraction was performed using a pre-trained VGG-face model. Facial features are focused on above the nose. The VGG-Face architecture consists of 1 Input layer, 13 convolutional layers (Conv), five max-pooling layers (Max-pool), and three fully connected (FC) layers. Two activation functions are used in the model architecture, namely Relu and SoftMax. The Relu activation function is used at the convolutional (Conv) and fully connected (FC) layers [30].



Fig. 4 VGG-face model architecture

A SoftMax activation function is used in the output or Prob layer. The VGG-face model is trained using the Labeled Faces in the Wild (LFW) dataset, consisting of 13,233 images with 5749 identities, and YouTube Faces, which contains 3425 videos of 1595 people collected from YouTube. The VGG-face architecture can be seen in Figure 4. The VGG-face model produces 2622 dimensional vectors that store facial features' embedding data, which are then carried out for identification [31].

C. Similarity Feature Distance

The Similarity Distance feature is a vector calculation between the input image and the image in the Database. Calculating the distance vector is to detect the difference between the input image and the image in the Database. The vector distance calculation is done by finding facial features That have been extracted previously using Euclidean distance. Euclidean distance is the shortest distance between two points in an N-dimensional space, also known as Euclidean space. The Euclidean distance calculation can be seen as follows [32].

$$d(p, q) = \sqrt{\sum_{i=1}^n (q_i - p_i)^2} \quad (1)$$

Where p, q are two points or points of Euclidean n . q_i, p_i are Euclidean vectors that start from the starting point. Before finding facial features, data sets, and input data, the vector normalization process is carried out first using the l2 norm. The l2 norm formula can be seen as follows [33].

$$|x| = \sqrt{\sum_{k=1}^n |X_k|^2} \quad (2)$$

Where $|X_k|$ show a complex modulus. The reason for vector normalization is that it makes features more consistent with each other so the model can make better predictions [34].

D. Temperature Measurement

The temperature measurement system carried out using the MLX90614 sensor is a contactless sensor that uses infrared for temperature measurement. The MLX90614 sensor has a measuring range from -40°C to 125°C [35]. The sensor is designed with NodeMCU ESP8266 [36]. The design of the temperature measurement system can be seen in Figure 5. The MLX90614 sensor needs to be recalibrated because it significantly differs from commercial thermometers when used directly. The sensor needs to be recalibrated to reduce the error rate. Sensor calibration is carried out using the Two-Point Calibration Method. Calibration Two Point Calibration will compare the sensor MLX90614 with a commercial infrared thermometer. The Two-Point Calibration method is used because the sensor output is linear in a range of values.

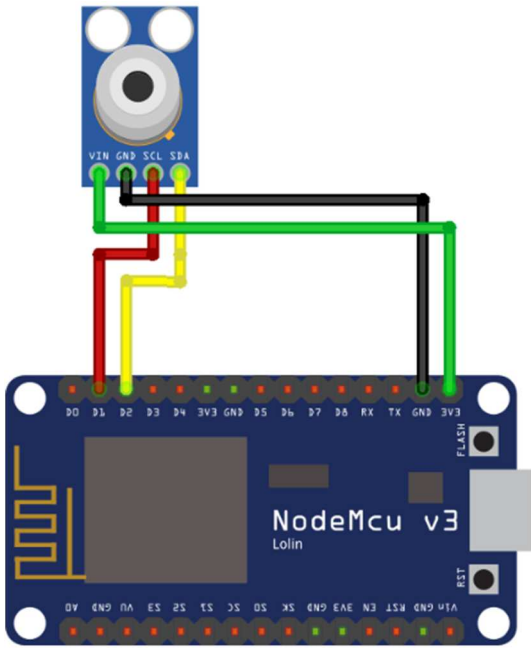


Fig. 5 Body temperature measurement system architecture using the NodeMCU ESP8266 sensor and Arduino Uno

III. RESULT AND DISCUSSION

A. Body Temperature Measuring Device

An attendance system is created using a smartphone camera as an image input tool. The smartphone is also paired with a temperature sensor. Figure 6 shows the results of the design of the tools used in the attendance system.



Fig. 6 Attendance tool for image capture and temperature measurement

B. Temperature measurement test

The temperature measurement test is carried out by directing the temperature measurement tool to the forehead area. The distance between the temperature measurement tool and the user is about 40-60 cm. The test is carried out in 2 stages: before measurement, before calibration, and after calibration. Table I shows the results of measuring body temperature before calibration. The test results in Table I show a significant enough difference with the comparison sensor before calibration is applied. The difference is reduced by performing a two-point calibration. The formula used for calibration is:

$$y = 2.0567x - 41.033 \quad (3)$$

Where y is the temperature input for calibration, the variables in the formula are obtained using a linear equation based on the measurement results in Table I. The

measurement results of the MLX90614 sensor with two-point calibration can be seen in Table II. The measurement result after calibration reduces the error rate to 0.1. Sensor testing after calibration was also carried out on five samples shown in Table III. The test results in Table III show that the sensor calibration was successfully carried out with an error rate of 0.1, the same as the results in Table II.

TABLE I
SENSOR TEST RESULTS BEFORE CALIBRATION

Subject	Sensor MLX90614	Thermometer infrared	Difference
1	34.1	36.6	2.5
2	33.9	36.5	2.6
3	34	36.4	2.4
4	34	36.5	2.5
5	34.6	36.8	2.2
6	34	36.4	2.4
7	33.6	36.4	2.8
8	33.9	36.5	2.6
9	34.5	36.6	2.1
10	34.4	36.6	2.2
Average difference			2.43

TABLE II
SENSOR TEST RESULTS AFTER CALIBRATION

Subject	Sensor MLX90614	Thermometer infrared	Difference
1	36.5	36.4	0.1
2	36.5	36.5	0
3	36.7	36.6	0.1
4	36.4	36.5	0.1
5	36.8	36.8	0
6	36.5	36.6	0.1
7	36.4	36.5	0.1
8	36.5	36.4	0.1
9	36.4	36.4	0
10	36.7	36.6	0.1
Average difference			0.07

TABLE III
SENSOR TEST RESULTS AFTER CALIBRATION WITH DIFFERENT SAMPLES

Subject	Thermometer Infrared	Sensor MLX90614	Difference
1	36.9	36.9	0.0
2	36.4	36.7	0.1
3	36.4	36.4	0.0
4	36.2	36.1	0.1
5	36.5	36.5	0.0
Average difference			0.15

C. Face Detection Test

Testing the face detection model begins with learning the detection model. The learning process is carried out by using 120 face images for the training process and 30 face images for the validation process. Each image used contains masked and unmasked faces of various sizes. The test was carried out with several differentiated scenarios based on the number of epochs and optimizers to determine the best epoch and optimizer for the face detection process. The learning outcomes of the model are described in Table IV. Based on Table IV, test scenarios using 300 Epoch and Adam's Optimizer resulted in the best and optimal value. Figures 7 to 10 show an evaluation graph based on classification loss, box loss, and object loss. Box loss represents how well the model can define and predict bounding boxes for objects, object loss

is the probability value that is in the region of interest, and classification loss represents how the model can predict the class correctly based on the detected object [37]. The test results show a decreasing trend in value along with the iteration, but it shows an increase in value in several iterations. This happens because the model fails to detect objects from the given image.

TABLE IV
FACE DETECTION MODEL LEARNING RESULTS

No.	Epoch	Optimizer	mAP_0.5	Precision	Recall	F1-Score
1	100	SGD	0.60	0.62	0.59	0.60
2	100	Adam	0.71	0.77	0.70	0.73
3	200	SGD	0.72	0.91	0.63	0.74
4	200	Adam	0.75	0.94	0.69	0.79
5	300	SGD	0.74	0.92	0.68	0.78
6	300	Adam	0.76	0.92	0.71	0.80
7	500	SGD	0.72	0.91	0.65	0.76
8	500	Adam	0.75	0.84	0.71	0.77

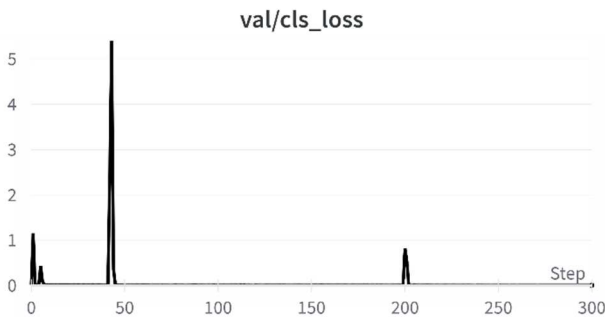


Fig. 7 Loss classification results when evaluating face detection models

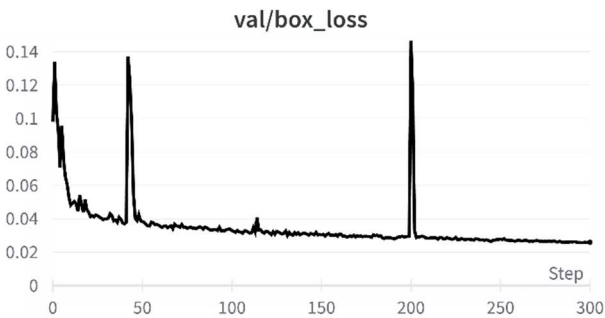


Fig. 8 Box loss results when evaluating face detection mode

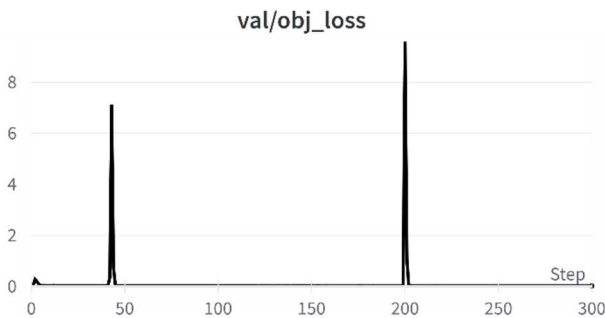


Fig. 9 Object loss results on face detection model evaluation

D. Face Identification Test

Facial identification test using LFW dataset. The test aims to identify faces with and without masks. The dataset was modified to use only a sample of 120 subjects. The Database used does not yet have a masked face sample, therefore, image augmentation is carried out to implement a mask on the sample face image [22]. The test begins with learning using the one-shot learning method, where this method only uses a few facial images from each sample for the learning process [38]. The learning process for testing uses five face images from each sample without a mask. The test results can be seen in Table V for testing samples without masks and Table VI for testing samples with masks.

The results of the face identification test without using a mask shown in Table V represent a fairly high level of accuracy. The result shows that VGG-Face can identify faces properly using only five training samples for each subject. The masked face identification test in Table VII shows a lower accuracy level than the test results in Table V. This is caused by the test image having noise in a mask utilized on the face. There are some types of masks used in face mask testing. They are cloth, surgical, N95, KN95, and gas masks. Using Norm L2 in testing provides a fairly good performance, where the test results in Table V show an increase of 2.86% and an increase of 3.11% percent from the test results in Table VI. This shows that using L2 Norm in the identification process can help improve the performance of the facial identification model.

TABLE V
FACE SUBJECT TEST RESULTS WITHOUT MASK

No.	Matrix	Score With Normalization	Score Without Normalization
1	Accuracy	93.10 %	90.24 %
2	Precision	93.82 %	91.43 %
3	Recall	93.10 %	90.24 %
4	F1-Score	92.89 %	90.12 %

TABLE VI
FACE SUBJECT TEST RESULTS WITH MASK

No.	Matrix	Score With Normalization	Score Without Normalization
1	Accuracy	54.23 %	51.12 %
2	Precision	67.82 %	65.50 %
3	Recall	54.23 %	51.12 %
4	F1-Score	54.00 %	50.34 %

E. Test attendance system

The attendance system test integrates facial identification and a human temperature measurement system. The test was conducted with 15 subjects from Indonesia with an age range of 17 – 22 years. Each subject is taken with as many as five images for the learning process. The subject image is taken at a distance of 40 – 60 cm from the camera and in various lighting conditions. The results of the facial identification test can be seen in the heatmap graphs in Figure 10 and Figure 11. The performance of the facial identification model is shown in Table VII. It shows that the facial identification model can carry out the identification process well, both for a face with a mask and without a mask. Identification testing of the masked face has a significant increase. Those are due to the use of training data that is good quality. Body temperature measurement tests were carried out on subjects in various

room conditions. The experimental results in Table VIII show the test results with the highest error rate of 0.2.

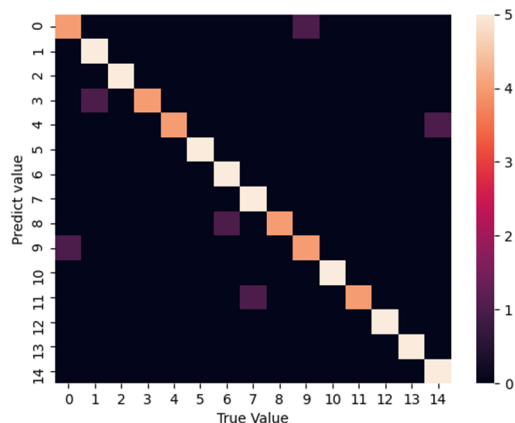


Fig. 10 Heatmap confusion matrix test subject without mask

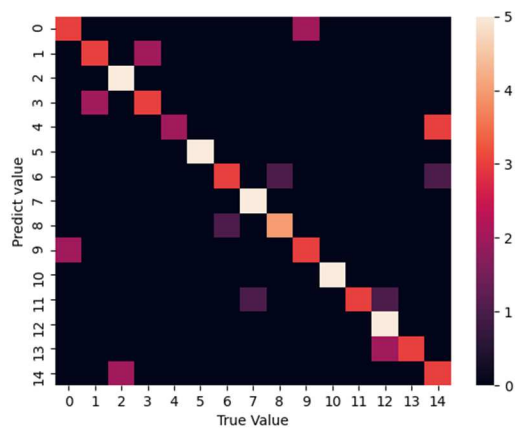


Fig. 11 Heatmap confusion matrix testing subject with mask

TABLE VII
FACE IDENTIFICATION TEST RESULTS

No.	Matrix	Subject with mask	Subject without mask
1	Accuracy	73.33 %	92.00 %
2	Precision	77 %	92.88 %
3	Recall	73.33 %	92.00 %
4	F1-score	72.99 %	91.94 %

TABLE VIII
SENSOR TEST RESULTS AFTER CALIBRATION WITH DIFFERENT SAMPLES

Subject	Thermometer Infrared	Sensor MLX90614	Difference
1	36.9	36.9	0.0
2	36.4	36.7	0.1
3	36.4	36.4	0.0
4	36.2	36.0	0.2
5	36.5	36.5	0.0
6	36.0	36.0	0.0
7	35.9	36.0	0.1
8	36.7	36.7	0.0
9	36.3	36.3	0.0
10	36.4	36.5	0.1
11	36.2	36.1	0.1
12	36.3	36.2	0.1
13	36.6	36.6	0.0
14	36.6	36.7	0.1
15	36.1	36.2	0.1
Average difference			0.07

IV. CONCLUSION

This paper proposes a system for preventing the spread of COVID-19. The system is an attendance system that can recognize masked faces and measure body temperature. Face identification utilizing the YOLO Framework achieved the highest F1-score score of 80% out of eight learning scenarios. This face detection model detects both masked and unmasked faces. VGG-Face is used for face feature extraction and generates a 2622-dimensional vector. This vector is then normalized using L2 to obtain more consistent features. The face identification process was evaluated using the LFW dataset, yielding an F1 score of 92.89% for faces without masks and 54% for faces with masks. This identification result was achieved after L2 normalized the features. The MLX90614 Sensor was calibrated to reduce error rates. The calibration technique is carried out by comparing the MLX90614 Sensor to other infrared thermometers. The error rate of the MLX90614 Sensor is 2.4° C before and 0.1° C after calibration. The developed attendance system combines the facial identification system and body temperature measurement. The test used 15 user samples. The identification process produced an F1 score of 91.94% for faces without masks and 72.99% for faces with masks. The face identification test's F1 score of the masked face increased due to numerous factors, including the picture quality. The temperature measurement system has a constant error rate of 0.1° C. This attendance system may be improved and utilized in various industries, including security and health care.

REFERENCES

- [1] J. Bedford *et al.*, "COVID-19: towards controlling of a pandemic," *Lancet*, vol. 395, no. 10229, pp. 1015–1018, 2020, doi: 10.1016/S0140-6736(20)30673-5.
- [2] Y. C. Wu, C. S. Chen, and Y. J. Chan, "The outbreak of COVID-19: An overview," *J. Chinese Med. Assoc.*, vol. 83, no. 3, pp. 217–220, 2020, doi: 10.1097/JCMA.0000000000000270.
- [3] F. Albarello *et al.*, "2019-novel Coronavirus severe adult respiratory distress syndrome in two cases in Italy: An uncommon radiological presentation," *Int. J. Infect. Dis.*, vol. 93, pp. 192–197, 2020, doi: 10.1016/j.ijid.2020.02.043.
- [4] X. Lv, L. Ding, and G. Zhang, "Research on fingerprint feature recognition of access control based on deep learning," *Int. J. Biom.*, vol. 13, no. 1, pp. 80–95, 2021, doi: 10.1504/IJBM.2021.112214.
- [5] S. Arya, N. Pratap, and K. Bhatia, "Future of Face Recognition: A Review," *Procedia Comput. Sci.*, vol. 58, pp. 578–585, 2015, doi: 10.1016/j.procs.2015.08.076.
- [6] A. Sepas-Moghaddam, A. Etemad, F. Pereira, and P. L. Correia, "CapsField: Light Field-Based Face and Expression Recognition in the Wild Using Capsule Routing," *IEEE Trans. Image Process.*, vol. 30, pp. 2627–2642, 2021, doi: 10.1109/TIP.2021.3054476.
- [7] M. Luo, J. Cao, X. Ma, X. Zhang, and R. He, "FA-GAN: Face Augmentation GAN for Deformation-Invariant Face Recognition," *IEEE Trans. Inf. Forensics Secur.*, vol. 16, pp. 2341–2355, 2021, doi: 10.1109/TIFS.2021.3053460.
- [8] J. Y. Choi and B. Lee, "Ensemble of Deep Convolutional Neural Networks with Gabor Face Representations for Face Recognition," *IEEE Trans. Image Process.*, vol. 29, no. c, pp. 3270–3281, 2020, doi: 10.1109/TIP.2019.2958404.
- [9] M. Awais *et al.*, "Novel Framework: Face Feature Selection Algorithm for Neonatal Facial and Related Attributes Recognition," *IEEE Access*, vol. 8, pp. 59100–59113, 2020, doi: 10.1109/ACCESS.2020.2982865.
- [10] H. Yang and X. Han, "Face recognition attendance system based on real-time video processing," *IEEE Access*, vol. 8, pp. 159143–159150, 2020, doi: 10.1109/ACCESS.2020.3007205.
- [11] X. Li, Z. Yang, and H. Wu, "Face detection based on receptive field enhanced multi-task cascaded convolutional neural networks," *IEEE*

- Access*, vol. 8, pp. 174922–174930, 2020, doi: 10.1109/ACCESS.2020.3023782.
- [12] N. V. Kousik, Y. Natarajan, R. Arshath Raja, S. Kallam, R. Patan, and A. H. Gandomi, “Improved salient object detection using hybrid Convolution Recurrent Neural Network,” *Expert Syst. Appl.*, vol. 166, p. 114064, 2021, doi: 10.1016/j.eswa.2020.114064.
- [13] S. Singh, U. Ahuja, M. Kumar, K. Kumar, and M. Sachdeva, “Face mask detection using YOLOv3 and faster R-CNN models: COVID-19 environment,” *Multimed. Tools Appl.*, 2021, doi: 10.1007/s11042-021-10711-8.
- [14] A. Kumar, A. Kalia, A. Sharma, and M. Kaushal, “A hybrid tiny YOLO v4-SPP module based improved face mask detection vision system,” *J. Ambient Intell. Humaniz. Comput.*, no. 0123456789, 2021, doi: 10.1007/s12652-021-03541-x.
- [15] R. Xu, H. Lin, K. Lu, L. Cao, and Y. Liu, “A forest fire detection system based on ensemble learning,” *Forests*, vol. 12, no. 2, pp. 1–17, 2021, doi: 10.3390/f12020217.
- [16] K. Lin *et al.*, “Face Detection and Segmentation Based on Improved Mask R-CNN,” *Discret. Dyn. Nat. Soc.*, vol. 2020, 2020, doi: 10.1155/2020/9242917.
- [17] S. Ampama, J. M. Kitayimbwa, and M. C. Were, “Performance of an open source facial recognition system for unique patient matching in a resource-limited setting,” *Int. J. Med. Inform.*, vol. 141, no. May, p. 104180, 2020, doi: 10.1016/j.ijmedinf.2020.104180.
- [18] V. Sunanthini *et al.*, “Comparison of CNN Algorithms for Feature Extraction on Fundus Images to Detect Glaucoma,” *J. Healthc. Eng.*, vol. 2022, 2022, doi: 10.1155/2022/7873300.
- [19] P. Peng, I. Portugal, P. Alencar, and D. Cowan, “A face recognition software framework based on principal component analysis,” *PLoS One*, vol. 16, no. 7, p. e0254965, Jul. 2021, doi: 10.1371/journal.pone.0254965.
- [20] S. Ben Chaabane, M. Hijji, R. Harrabi, and H. Seddik, “Face recognition based on statistical features and SVM classifier,” *Multimed. Tools Appl.*, vol. 81, no. 6, pp. 8767–8784, 2022, doi: 10.1007/s11042-021-11816-w.
- [21] A. Alzu’bi, F. Albalas, T. Al-Hadhrani, L. B. Younis, and A. Bashayreh, “Masked face recognition using deep learning: A review,” *Electron.*, vol. 10, no. 21, 2021, doi: 10.3390/electronics10212666.
- [22] H. Deng, Z. Feng, G. Qian, X. Lv, H. Li, and G. Li, “MFCosface: A Masked-Face Recognition Algorithm Based on Large Margin Cosine Loss,” *Appl. Sci.*, vol. 11, no. 16, p. 7310, Aug. 2021, doi: 10.3390/app11167310.
- [23] N. Ud Din, K. Javed, S. Bae, and J. Yi, “A Novel GAN-Based Network for Unmasking of Masked Face,” *IEEE Access*, vol. 8, pp. 44276–44287, 2020, doi: 10.1109/ACCESS.2020.2977386.
- [24] N. S. Rafa *et al.*, “IoT-Based Remote Health Monitoring System Employing Smart Sensors for Asthma Patients during COVID-19 Pandemic,” *Wirel. Commun. Mob. Comput.*, vol. 2022, 2022, doi: 10.1155/2022/6870358.
- [25] P. Dolibog, B. Pietrzyk, K. Kierszniok, and K. Pawlicki, “Comparative Analysis of Human Body Temperatures Measured with Noncontact and Contact Thermometers,” *Healthc.*, vol. 10, no. 2, 2022, doi: 10.3390/healthcare10020331.
- [26] A. A. Rahimoon, M. N. Abdullah, and I. Taib, “Design of a contactless body temperature measurement system using Arduino,” *Indones. J. Electr. Eng. Comput. Sci.*, vol. 19, no. 3, p. 1251, Sep. 2020, doi: 10.11591/ijeecs.v19.i3.pp1251-1258.
- [27] N. W.-J. Goh *et al.*, “Design and Development of a Low Cost, Non-Contact Infrared Thermometer with Range Compensation,” *Sensors*, vol. 21, no. 11, p. 3817, May 2021, doi: 10.3390/s21113817.
- [28] W. Xia, J. Yan, and Y. Li, “STM32-Based Contactless Temperature Measurement and Identification Device,” *IOP Conf. Ser. Earth Environ. Sci.*, vol. 692, no. 2, p. 022041, Mar. 2021, doi: 10.1088/1755-1315/692/2/022041.
- [29] Q. Xu, Z. Zhu, H. Ge, Z. Zhang, and X. Zang, “Effective Face Detector Based on YOLOv5 and Superresolution Reconstruction,” *Comput. Math. Methods Med.*, vol. 2021, 2021, doi: 10.1155/2021/7748350.
- [30] K. H. Cheah, H. Nisar, V. V. Yap, C. Y. Lee, and G. R. Sinha, “Optimizing residual networks and vgg for classification of eeg signals: Identifying ideal channels for emotion recognition,” *J. Healthc. Eng.*, vol. 2021, 2021, doi: 10.1155/2021/5599615.
- [31] J. Tian, H. Xie, S. Hu, and J. Liu, “Multidimensional Face Representation in a Deep Convolutional Neural Network Reveals the Mechanism Underlying AI Racism,” *Front. Comput. Neurosci.*, vol. 15, no. March, pp. 1–8, Mar. 2021, doi: 10.3389/fncom.2021.620281.
- [32] Z. Hu and Y. Wang, “Multiclass Interactive Martial Arts Teaching Optimization Method Based on Euclidean Distance,” *Secur. Commun. Networks*, vol. 2022, 2022, doi: 10.1155/2022/7272048.
- [33] L. Yu and X.-S. Gao, “Improve Robustness and Accuracy of Deep Neural Network with L_{2,∞} Normalization,” *J. Syst. Sci. Complex.*, vol. 36, no. 1, pp. 3–28, 2023, doi: 10.1007/s11424-022-1326-y.
- [34] P. Huang, Q. Ye, F. Zhang, G. Yang, W. Zhu, and Z. Yang, “Double L_{2,p}-norm based PCA for feature extraction,” *Inf. Sci. (Ny)*, vol. 573, pp. 345–359, Sep. 2021, doi: 10.1016/j.ins.2021.05.079.
- [35] S. R. Anan, M. A. Hossain, M. Z. Milky, M. M. Khan, M. Masud, and S. Aljahdali, “Research and Development of an IoT-Based Remote Asthma Patient Monitoring System,” *J. Healthc. Eng.*, vol. 2021, 2021, doi: 10.1155/2021/2192913.
- [36] K. Islam, F. Alam, A. I. Zahid, M. M. Khan, and M. Inamabbasi, “Internet of Things- (IoT-) Based Real-Time Vital Physiological Parameter Monitoring System for Remote Asthma Patients,” *Wirel. Commun. Mob. Comput.*, vol. 2022, 2022, doi: 10.1155/2022/1191434.
- [37] M. Kasper-Eulaers, N. Hahn, S. Berger, T. Sebulonsen, Ø. Myrland, and P. E. Kummervold, “Short Communication: Detecting Heavy Goods Vehicles in Rest Areas in Winter Conditions Using YOLOv5,” *Algorithms*, vol. 14, no. 4, p. 114, Mar. 2021, doi: 10.3390/a14040114.
- [38] K. Yoon, J. Gwak, Y. M. Song, Y. C. Yoon, and M. G. Jeon, “OneShotDA: Online Multi-Object Tracker with One-Shot-Learning-Based Data Association,” *IEEE Access*, vol. 8, pp. 38060–38072, 2020, doi: 10.1109/ACCESS.2020.2975912.